



저작자표시-비영리-변경금지 2.0 대한민국

이용자는 아래의 조건을 따르는 경우에 한하여 자유롭게

- 이 저작물을 복제, 배포, 전송, 전시, 공연 및 방송할 수 있습니다.

다음과 같은 조건을 따라야 합니다:



저작자표시. 귀하는 원저작자를 표시하여야 합니다.



비영리. 귀하는 이 저작물을 영리 목적으로 이용할 수 없습니다.



변경금지. 귀하는 이 저작물을 개작, 변형 또는 가공할 수 없습니다.

- 귀하는, 이 저작물의 재이용이나 배포의 경우, 이 저작물에 적용된 이용허락조건을 명확하게 나타내어야 합니다.
- 저작권자로부터 별도의 허가를 받으면 이러한 조건들은 적용되지 않습니다.

저작권법에 따른 이용자의 권리는 위의 내용에 의하여 영향을 받지 않습니다.

이것은 [이용허락규약\(Legal Code\)](#)을 이해하기 쉽게 요약한 것입니다.

[Disclaimer](#)

이학석사 학위논문

녹내장성 마우스 모델 DBA/2J의
비정상적 안구 형태변화와
실험모델로서의 적합성

Abnormal Ocular Morphological Changes in the
Glaucomatous Mouse Model DBA/2J
and its Suitability as an Experimental Model

울산대학교 대학원

의과학과

김정훈

녹내장성 마우스 모델 DBA/2J의
비정상적 안구 형태변화와
실험모델로서의 적합성

Abnormal Ocular Morphological Changes in the
Glaucomatous Mouse Model DBA/2J
and its Suitability as an Experimental Model

지도교수 이주용

이 논문을 이학석사 학위논문으로 제출함

2024년 2월

울산대학교 대학원

의과학전공

김정훈

김정훈의 이학석사 학위논문을 인준함

심사위원 이 주 용 인

심사위원 황 창 모 인

심사위원 성 영 훈 인

울산대학교 대학원

2024년 2월

Abstracts

Glaucoma is a degenerative disease of the optic nerve associated with abnormal intraocular pressure, linked to the abnormal production and outflow of aqueous humor circulating within the eye. If the amount generated becomes abnormally excessive or if the drainage angle is blocked, leading to a significant increase in intraocular pressure, degeneration occurs in the retinal layers and the optic nerve. Particularly, damage is known to occur in the layer of nerve cells. Globally, it has an incidence rate of approximately 3.54% between the ages of 40 and 60.

Prior to conducting experiments on glaucoma, we aimed to perform a phenotype analysis of DBA/2J, which serves as the experimental group. Previously reported characteristics in this strain include iris atrophy and depigmentation, closure of the anterior chamber angle, abnormally increased intraocular pressure (IOP) speculated to be due to these changes, and subsequent degeneration of glaucomatous retinal layers, all occurring between 3 and 6 months of age. DBA/2N from the same lineage was used as the control group, and observations were made from 1 to 15 months of age.

Various observations were conducted to confirm the expression of these phenomena. These included observations of iris atrophy and depigmentation through anterior segment photography, intraocular pressure measurement using a tonometer, observations of the anterior chamber angle and retinal layers using optical coherence tomography (OCT) and electroretinography (ERG), and observations of changes in retinal inner layer thickness using H&E histological staining.

The results of the experiments showed clear changes in anterior segment photography. In DBA/2J, changes in the iris began to appear after 3 months, with abnormal thickening of the outer edge of the iris or gradual disappearance of changes in pupil size. Additionally, changes due to depigmentation, speculated to be caused by inflammation, led to interference in subsequent observations. Intraocular pressure data obtained from individuals exhibiting such changes also showed a clear difference from the control group (IOP mean in both eyes at 15 months: DBA/2N approximately 12.3 mmHg, DBA/2J 17.3 mmHg). OCT data confirming the closure of the anterior chamber angle performed later also showed clearer results in the experimental group. However, other tests performed did not reveal significant differences.

ERG showed no significant differences in the values of both a-wave and b-wave between the experimental and control groups (at 12 months, a-wave - DBA/2J: -56.9 ± 32.8 , DBA/2N: -56.9 ± 6.3 / b-wave - DBA/2J: 91.7 ± 37.7 , DBA/2N: 94.7 ± 30.4). While some changes were observed in the overall thickness of the retina with age, changes in the inner retinal layers were not clearly visible. Age-related changes were not distinct in the results of H&E histological staining.

In conclusion, the expression of glaucomatous symptoms in DBA/2J appeared to be somewhat consistent. These symptoms included iris atrophy, depigmentation, and closure of the anterior chamber angle, resulting in an increase in IOP. However, as previously reported, results regarding degeneration, such as changes in the thickness of the ganglion cell layer in the inner retina, did not show significant differences. Additionally, issues affecting the experiments were observed in the changes in the anterior segment, such as

blockage of the pupil due to depigmentation. Particularly, changes in the cornea occurred near the center of the eye, leading to conditions such as the formation of blood vessels, resulting in obstruction of the pupil and interference in IOP measurements. Some individuals with blocked pupils made observations through devices such as OCT and ERG impossible. Therefore, additional research is deemed necessary for the study of glaucomatous diseases in DBA/2J.

Table of Contents

1. Abstracts

2. Introduction

3. Methods

- **Animals**
- **Anesthesia**
- **Anterior Chamber Observation**
- **IOP Measurement**
- **Fundus and OCT**
- **Retinal Thickness Analysis**
- **ERG**
- **H&E Staining**

4. Results

- **External Ocular Imaging: Observation of Anterior Chamber Morphological Changes**
- **IOP Measurements**
- **Fundus Imaging and OCT: Structural Changes in Anterior Segment and Retina**
- **Retinal Thickness Analysis**
- **Confirmation of Validity in the Experimental Group from ERG and H&E Staining**

5. Conclusion

6. References

7. 국문 초록

Introduction

Glaucoma is a highly prevalent disease, primarily associated with aging, with an incidence rate of approximately 3.54% between the ages of 40 and 80.^{1,2} There is currently no effective treatment for the worsening symptoms that occur after glaucoma occurrence. Early intervention is possible, but delaying it can lead to significant damage, especially in the ganglion cell layer (GCL) of the retinal layer, resulting in degradation.³⁻⁵

Glaucoma occurs due to abnormal increases in intraocular pressure (IOP), caused by disturbances in the production and outflow of aqueous humor. Aqueous humor is secreted by the ciliary body, filling both the anterior and posterior chambers before draining through the trabecular meshwork. Glaucoma can occur in two primary causes: (i) abnormal production of aqueous humor, and (ii) abnormal efflux of aqueous humor because of blockage the trabecular meshwork in the anterior segment where aqueous humor exits. In these cases, they both result in increased IOP. The worsening of this phenomenon can be attributed to these conditions, which occurs due to the expansion force of the aqueous humor trying to escape from the eye and the resistance of the sclera trying to maintain the eye's volume. As a result, external stress is exerted on the retina, located in the middle of two counter sides of the eye, leading to ganglion cell layer (GCL) loss.

DBA/2J mice, a strain within the DBA2 lineage, are commonly used as an experimental group for glaucoma research, as they exhibit symptoms similar to glaucoma in humans⁶. Their glaucomatous response leans towards the blockage of trabecular meshwork, and these changes are reported to be reasoned by inflammatory responses⁷⁻⁸. We aimed to conduct various measurements in the methods of many types of imaging and data analysis

on the symptoms exhibited by DBA/2J as a glaucoma disease model. These measurements included anterior chamber observation, IOP measurements, fundus examination, optical coherence tomography (OCT), and electroretinography (ERG).

The glaucoma mouse model, while demonstrating some symptoms that are similar to humans, is not yet in a fully established state. In this situation, we set out to address the lack of research utilizing multi-imaging methods on the DBA/2N and DBA/2J strains, where comprehensive reports were not published.

Methods

Animals

We obtained and used DBA/2J mice as the experimental group from The Jackson Laboratory, with DBA/2N mice used as the control group. Both groups share the common DBA2 strain. Due to a higher reported incidence rate in female DBA/2J mice, we chose to observe and analyze female individuals. All animals from both groups were maintained in the same environment, receiving identical food and water supplies. Glaucoma onset in the experimental group typically occurs after 4 months of age, so we focused our experiments on this period and the months preceding and following it. When comparing individuals between the groups, control group DBA/2N and experimental group DBA/2J, were age-matched.

Anesthesia

For mouse experiments, we anesthetized them using a mixture of alfaxalone (Alfaxan, 0.8 mL/kg; JUROX Pty Ltd, Rutherford, NSW, Australia) and xylazine (Rompun, 0.2 mL/kg; Bayer Korea Ltd., Seoul, Republic of Korea) in a 4:1 ratio, adjusted based on body weight, age, and health. Injections were administered using a 1mL syringe (Sterile Hypodermic Syringe 1mL, Korea Vaccine Co., LTD., Republic of Korea) or insulin syringe (BD Ultra-Fine 1mL, Becton-Dickinson, USA). The injection volume was approximately 1/50 of the body weight for each individual. Adjustments were made for individual health conditions, with the first anesthesia using a slightly lower dose for some individuals to prevent shock. Post-

experiment care was provided based on the animals' conditions.

Anterior Chamber Observation

In the observations of the experimental group, the first experimental work was given to observing changes in the anterior chamber. We used a microscopic camera and its accompanying software for this purpose. Images were captured with the pupils at the center of the field of view, and observations were conducted in approximately two divisions around the pupils and the central area of the eye. The resolution was approximately 40x, and images were aligned based on the pupils and areas of abnormality. This camera also allowed us to examine the condition of the cornea. The conformational changes in the anterior segment were particularly focused on during OCT and fundus.

IOP measurement

IOP measurements were taken using the iCARE TONOLAB (iCare LAB, iCare Finland Oy, Finland). To address the variations in IOP depending on time zone, measurements were consistently taken between 12 pm and 2 pm⁹. Adequate cares were taken to minimize any interference from the mouse's head movements.⁸ Measurements were taken monthly based on the DOB of the mice. As IOP values can vary depending on the individual's condition, we took measurements more than five times for each animal and selected approximately 10 readings with minimal variation to calculate the average and standard deviation. Data was processed in this manner to account for variations in individual

conditions, especially as we observed some animals might exhibit shock. Data was collected every month until 15 months, aiming to capture observations in each age category. Individuals with no corneal abnormalities can be tested according to the original protocol (Figure 1. A). However, in cases where such abnormalities are present, measurements must be taken slightly off-axis since the probe cannot make direct contact with the pupil (Figure 1. B.).

Fundus and OCT

For the observation of changes in the anterior segment, particularly in the iris, we used a Phoenix Fundus camera IV connected to an Image-Guided OCT2 (Pheonix). Fundus images were captured to observe the overall appearance of the anterior chamber. Additionally, given the symptoms related to the iris and pupil in glaucoma, we conducted transillumination using a camera that projects light directly into the pupils, reflecting off the retina. OCT involved two types of imaging, focusing on the anterior segment, including the iris, cornea, pupil, and sclera (AS-OCT), and retinal layers and the optic nerve (retinal OCT). These observations were conducted to be measured on at 1 month age, and after then, once in every 3 months.

Retinal Thickness Analysis

Using the data obtained from retinal OCT, we conducted data analysis of retinal thickness changes. Since GCL was reported to exhibit changes in glaucoma, our primary goal was to

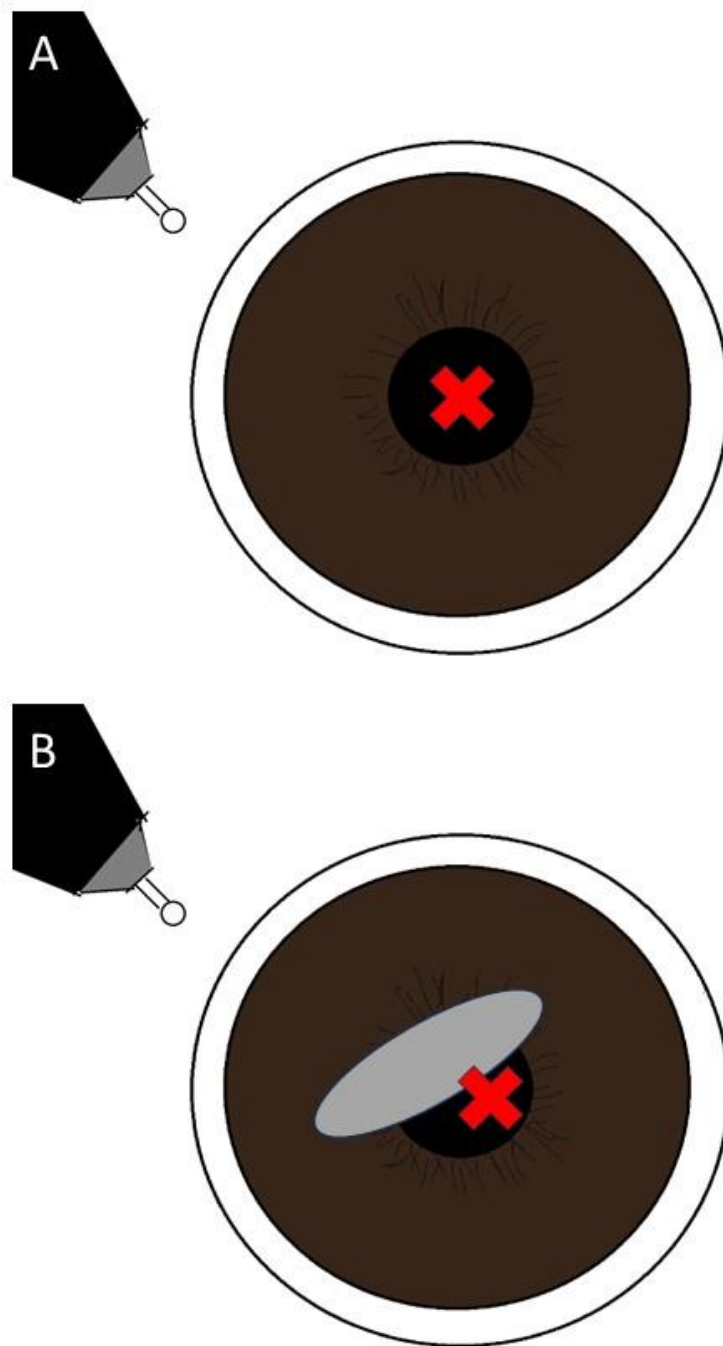


Figure 1. The targeting point for measurement of IOP by using rebound tonometer. In the case of having normal corneal conditions of experimental mice, we targeted the center of pupil(A). Besides, mice showing abnormality on cornea, we deflected to the points maintained on the pupil of the eyes of mice(B).

observe GCL. Unfortunately, precise GCL observations were not attainable, so we substituted it with analyzing changes in the thickness of the inner retinal layers. We graphed and recorded the thickness of each layer for analysis. Data were collected and compared for each group, based on age in months, with monthly data collection from 1 month to 6 months and then every 3 months after.

ERG

For ERG data collection, we induced dark adaptation in the mice for over 12 hours¹¹. All ERG measurements were conducted using the Phoenix Micron IV system and processed with LabScribeERG software (Phoenix Research Labs). Given that rod cell responses are predominantly observed in mice, we focused on rod cell responses and set the light intensity at log cd. We compared the a-wave and b-wave data obtained in both the DBA/2J experimental group and the DBA/2N control group. Data were collected from 1 month of age, with data points every 3 months.

H&E Staining

For both the experimental and control groups, we extracted eye samples through perfusion, followed by paraffin embedding and cutting mainly around the optic nerve. Subsequently, we conducted H&E staining and obtained microscopic images showing the various layers. The comparison of data between the two groups was performed, as with the retinal layer thickness analysis. The data were collected using the same criteria as for

retinal layer thickness analysis. The samples were gained every month until 6 months age and after then, once in every 3 months.

Results

External Ocular Imaging: Observation of Anterior Chamber Morphological Changes

During external ocular imaging, we observed morphological changes suggestive of iris atrophy in DBA/2J individuals, compared with DBA/2N ones (Figure 2)¹²⁻¹³. On A-F on the figure which shows the conformations of DBA/2J eyes, retinal changes included thickening of the iris border and pigment dispersion, probably due to inflammation¹³⁻¹⁶. In some cases, pigment dispersion was so severe that it almost completely covered the pupils. Moreover, the position of the pupils was often off-center.

While similar changes were absent in the control group (DBA/2N), the DBA/2J group exhibited these morphological changes mainly around 3 months before and after birth, with increasing severity as they aged.

However, both the experimental and control groups exhibited abnormal changes in the cornea (Figure 3)¹². These changes appeared primarily after 1 month age and seemed to start as small, white scars. However, they progressed to the extent of developing blood vessels and other changes over time.

IOP Measurements: Dynamic Trends in Intraocular Pressure

The IOP measurements consistently revealed higher pressures in the DBA/2J group than in the control group (Figure 4). As shown in the graphs and tables, these increased pressures started to show significant differences after 3 months of age. The pressure consistently increased as the individuals aged in both groups. However, control group

(DBA/2N) mice displayed relatively stable IOP over time, while DBA/2J mice exhibited a progressive rise, reaching alarming levels as they approached 14-15 months of age. In the 15 months age, IOP of DBA/2J were measured about 17.3 mmHg and that of DBA/2N 12.3 mmHg in average values of two other side eyes. The values we gathered were relatively lower than Wang referred, however, they might show DBA/2J tested in our research also occurred glaucomatous symptoms ¹⁰.

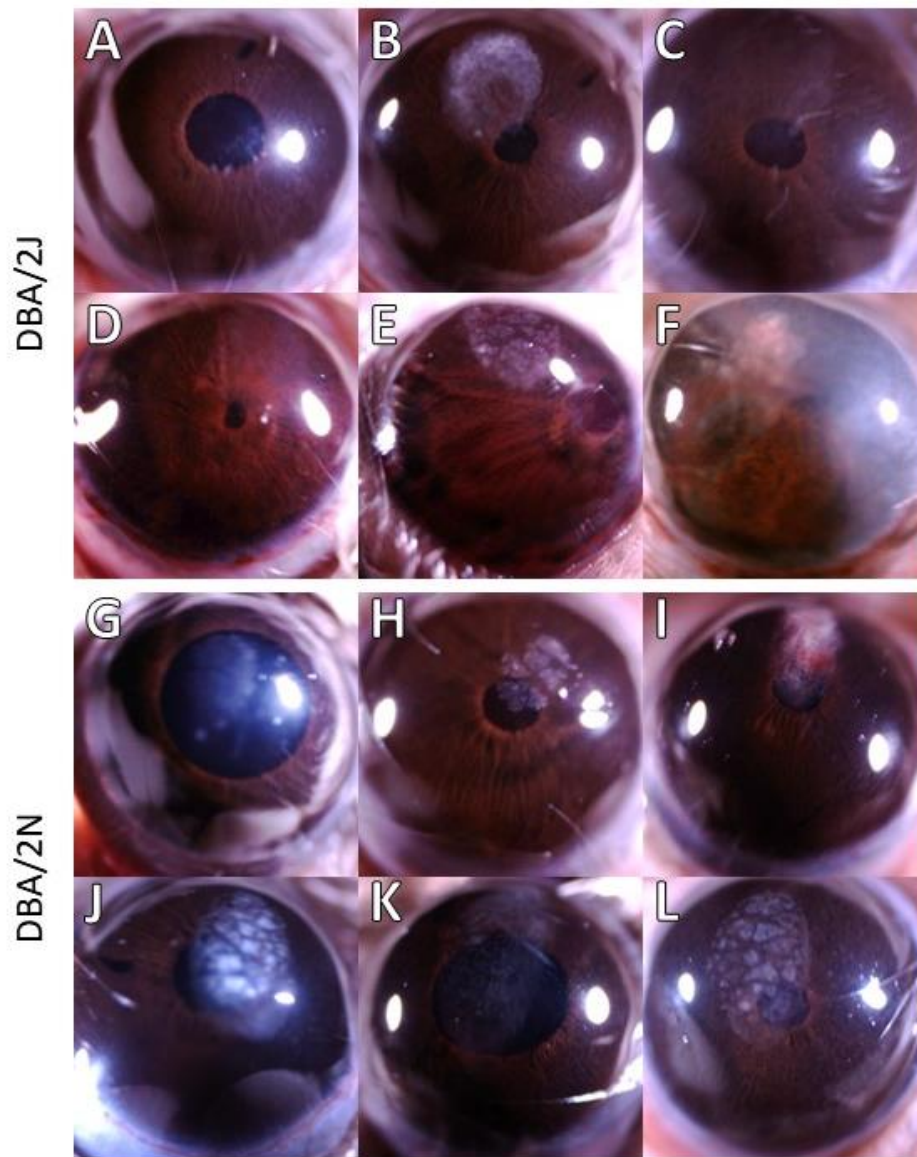


Figure 2. The changes of iris of each group. A-F show the outer conformations of anterior segment in DBA/2J (A: 1M, B: 3M, C: 6M, D: 9M, E: 12M, 15M) and G-L are them of DBA/2N (G: 1M, H: 3M, I: 6M, J: 9M, K: 12M and L: 15M). The anterior segments of DBA/2J were blurred by dispersed pigments in some individuals

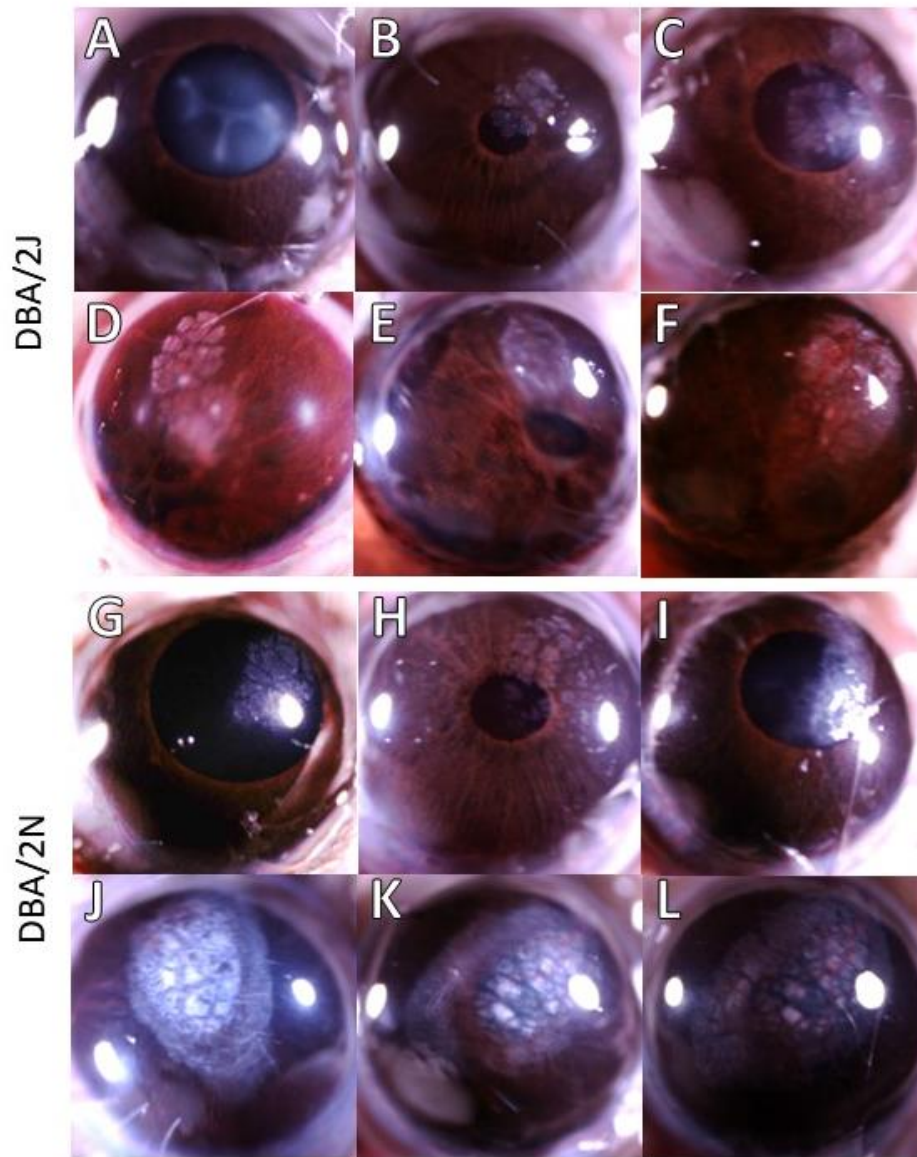


Figure 3. The images showing changes of cornea of each group. A-F show the outer conformations of anterior segment in DBA/2J (A: 1M, B: 3M, C: 6M, D: 9M, E: 12M, 15M) and G-L are them of DBA/2N (G: 1M, H: 3M, I: 6M, J: 9M, K: 12M and L: 15M). Both groups exhibited abnormal changes in the cornea, primarily occurring around the center of the eye and the periphery of the pupil. When these changes worsened, they often interfered with the process of obtaining data from the retina through the pupil.

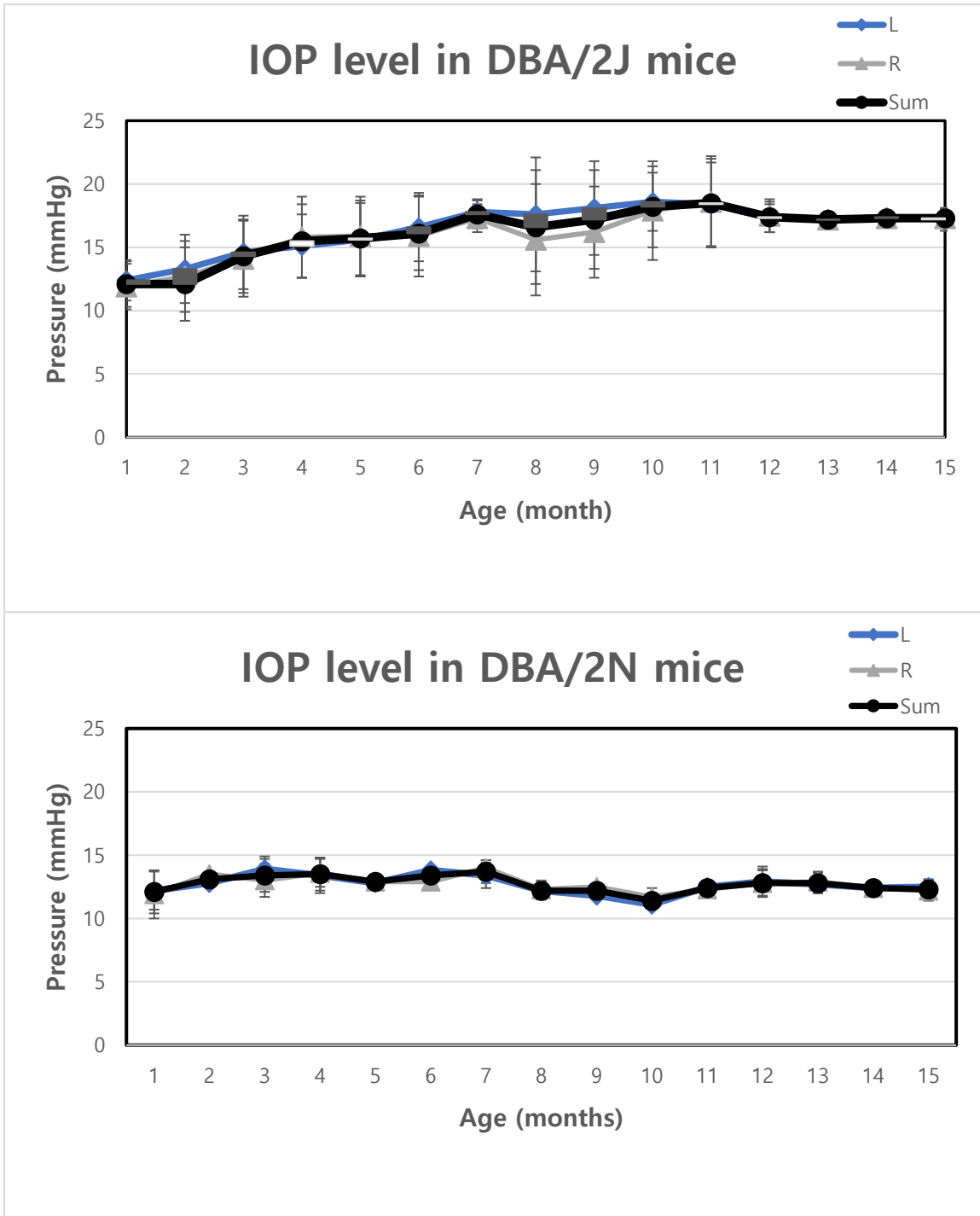


Figure 4. The graphs and values of IOP in the DBA/2N and DBA/2J mice eyes. The graphs on the left side shows the results of IOP measurement on each other groups. As previously reported, an increase in IOP was clearly evident when compared to DBA/2N, especially 4 months before and after.

Fundus Imaging and OCT: Structural Changes in Anterior Segment and Retina

Fundus imaging showed evident structural changes in the anterior segment of the eyes in DBA/2J mice. These changes included iris atrophy, pupil dilation, and pigment dispersion, which were observed by transillumination photography (Figure 5) ¹². Such changes were absent in the control group. Anterior segment optical coherence tomography (AS-OCT) revealed a consistent thickening of the anterior segment layers, particularly the iris and cornea, in DBA/2J mice (Figure 6). In image A of figure 5, iris is shown as if swelling and abnormal conformation is formed, while B shows normal iris. The anterior angle of eyes of DBA/2J in 10 months age were closed, in spite of maintenance of open angle in DBA/2N mice in same age (Figure 5). Furthermore, as depicted in Figure 7, it was observed that in DBA/2J, the drainage angle was not blocked at 1 month of age, but a pattern of blockage was observed at 15 months of age.

However, in DBA/2J, morphological changes occurred in two ways; one was an increase in the separation between the iris and cornea (Figure 8. B.), and the other was adhesion between these two areas (Figure 8.C.). These phenomena were guessed as the results of inflammatory symptoms.

Retinal Thickness Analysis

Retinal OCT data analysis didn't show significant differences in retinal thickness between the two groups (Figure 9 and Table 2 and 3). The inner retinal layers, mainly the ganglion cell layer (GCL) and inner plexiform layer (IPL), displayed marked thinning in DBA/2J mice

as they aged. This thinning was consistent with glaucoma-related damage. The control group, on the other hand, showed no significant change in these layers (Table 2 and 3). Furthermore, during the stage of conducting retinal OCT, the previously mentioned abnormal responses became a limiting factor, significantly reducing the number of individuals from which data could be extracted.

Confirmation of Validity in the Experimental Group from ERG and H&E Staining

When comparing the a-wave and b-wave in the ERG data, there is some variation between DBA/2J and DBA/2N (Figure 10). In 6 months after birth, the wave points of a-wave and b-wave in DBA/2J and DBA/2N had the most different values (a-wave: -56.2 ± 12.6 (DBA/2J) vs -75.1 ± 25.8 (DBA/2N); b-wave: 91.4 ± 22.1 (DBA/2J) vs 107.9 ± 44.2 (DBA/2N) and their units are same, $\log \text{cd/m}^2$). However, given that this pattern did not consistently appear in all individuals with ocular changes, further validation is needed to establish the efficacy of the experimental group since 12 months age (a-wave: -56.9 ± 32.8 (DBA/2J) vs -56.9 ± 6.3 (DBA/2N); b-wave: 91.7 ± 37.7 (DBA/2J) vs 94.7 ± 30.4 (DBA/2N) and their units are same, $\log \text{cd/m}^2$).

Similarly, in H&E staining, significant differences were not readily apparent. Comparing the experimental and control groups at various ages, thickness variations were not highly (Figure 11). These results indicate that the changes in each retinal layer were not visibly apparent. Consequently, contrary to our expectations, DBA/2J may not exhibit significant ganglion cell layer (GCL) loss as a glaucoma model.

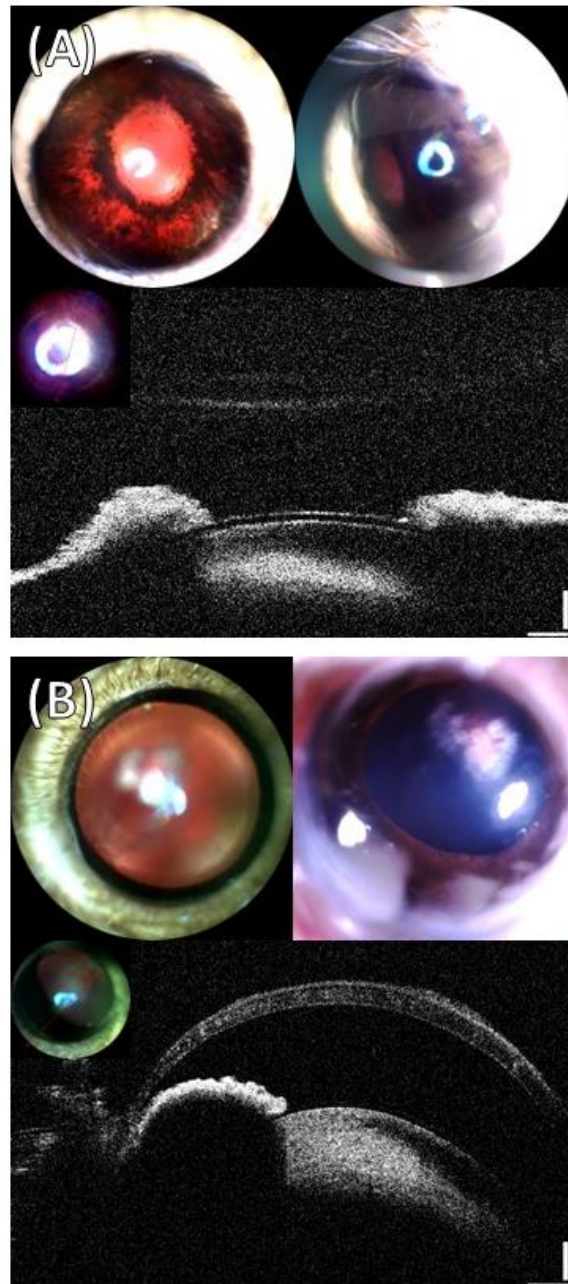


Figure 5. The images of anterior segment and AS-OCT from the DBA/2J (A; 10 months age) with iris atrophy and the DBA/2N (B; 10 months age). These image shows the configuration of iris atrophy in DBA/2J compared with the control group. As shown in this figure, the shape of the iris appears to exhibit a distinct pattern of swelling and an irregular texture, contrasting with the age-matched control group.

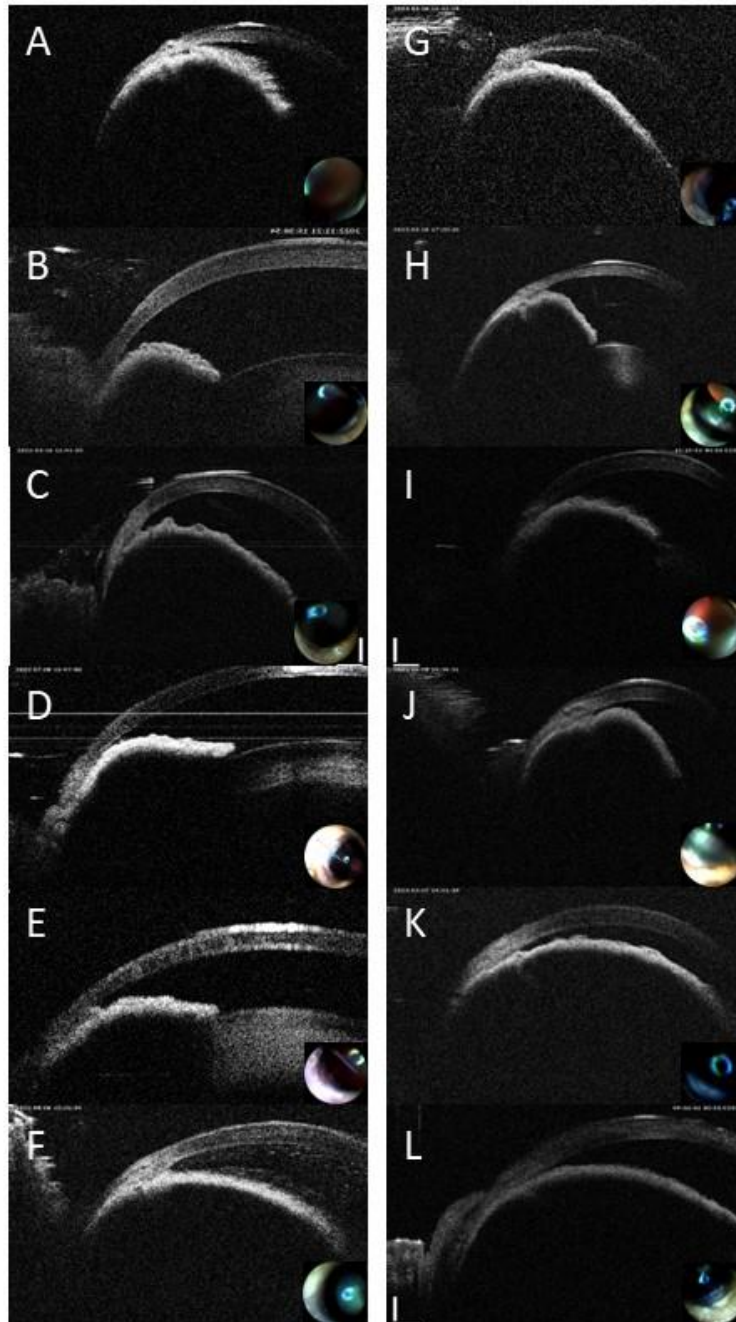


Figure 6. A-F is AS-OCT data from experimental group DBA/2J (each as 1-6 months ages in order) and G-L is them from control group DBA/2N (same as former). As shown in the images, with increasing age, the symptoms of gradual angle closure at the cornea-iris junction, specifically in the region of the scleral spur, were occurred.

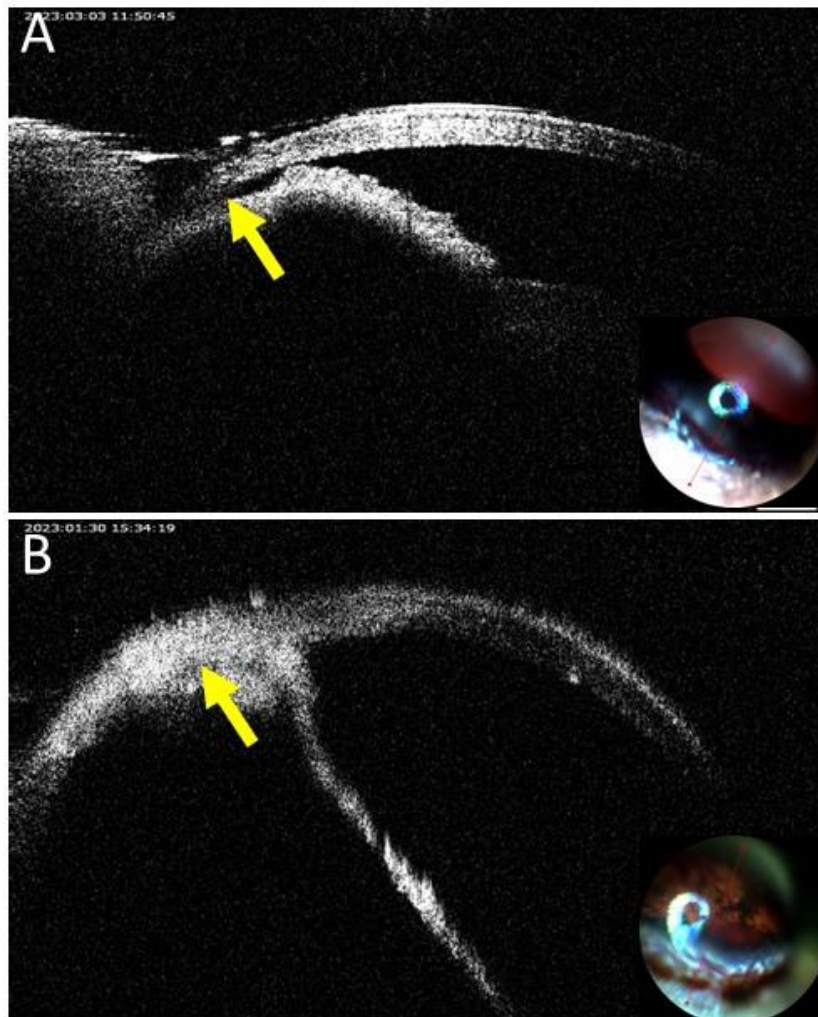


Figure 7. Anterior angle of DBA/2J in the side inferior one. A is from 1 month age, and B is from 15 months ages. The yellow arrows aim to point at the area near the scleral spur. Individuals with 1 month age had empty or open anterior angle, while their elders, especially with increasing age, the anterior angles tended to exhibit a more comparable degree of closure.

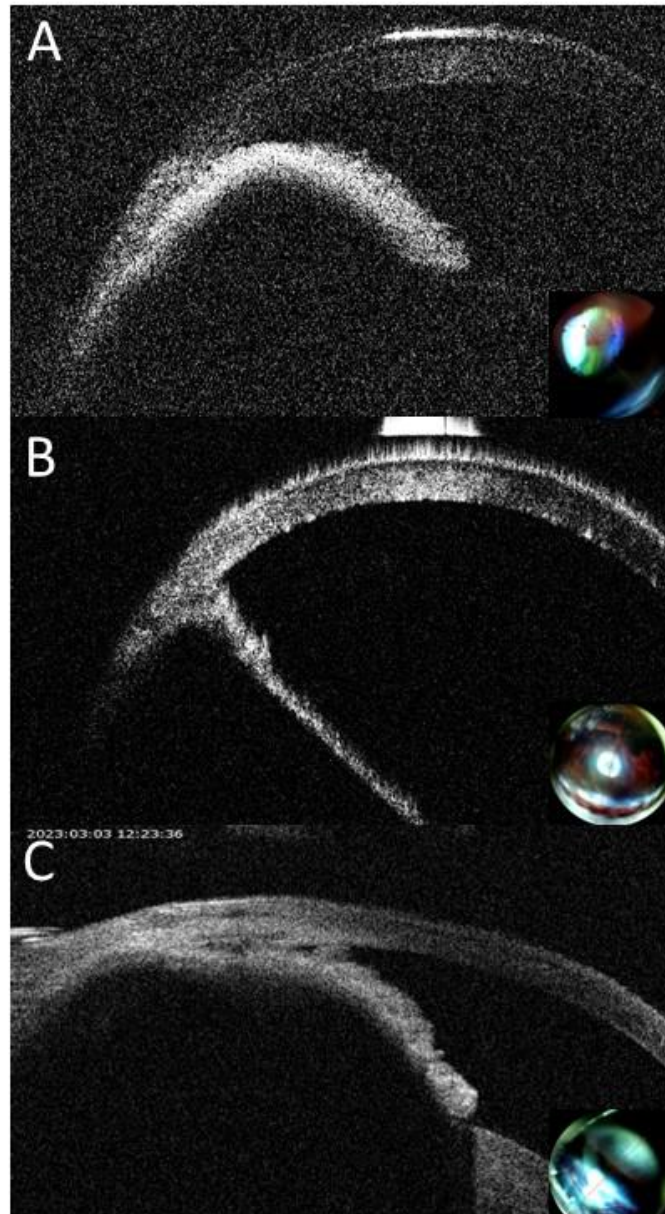


Figure 8. Two types of abnormal changes of anterior chamber. They are the AS-OCT from the anterior side. A is image of DBA/2N, each B and C is those of DBA/2J. B shows broadened depth between iris and cornea, because of swelling. On the other hand, C appeared to be attached to each other because the distance between the iris and the cornea was very close.

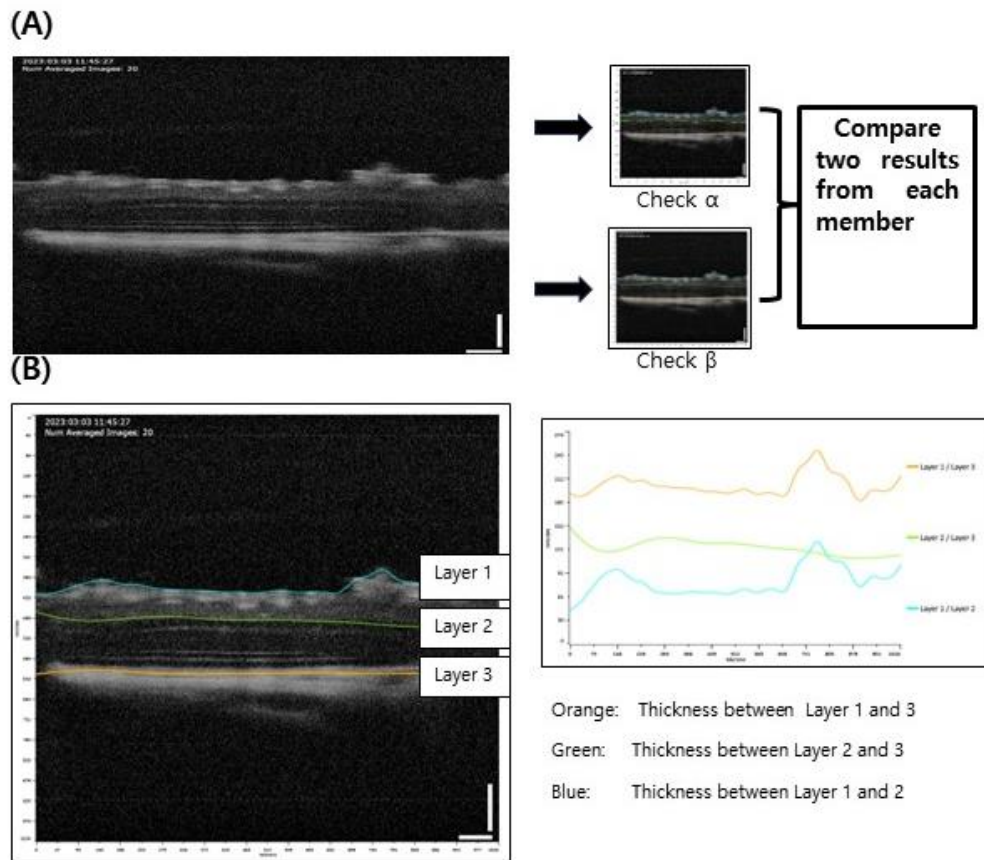


Figure 9. Retinal thickness analysis standards(A) and average retinal thickness crosscheck sheets (B: inner retinal layer; C: total retinal layer). In contrast to the pronounced differences observed in the anterior segment, changes in retinal thickness seemed less statistically significant or difficult to ascertain.

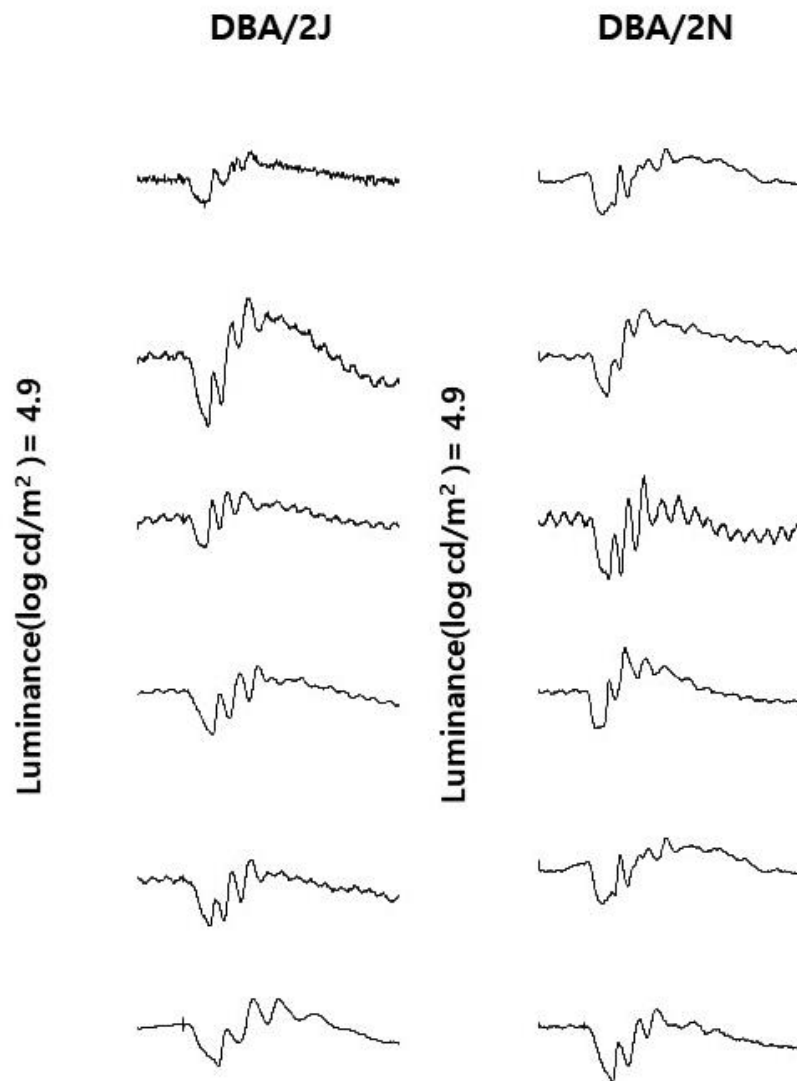


Figure 10. The ERG graph from rod cells in DBA/2J and DBA/2N mice and average values of b-wave and a-wave. These data wasn't show significant differences between DBA/2J and DBA/2N. As they are shown, the values from two other groups have trends that their different values were going to be bigger, commensurate with ages. However, the individuals beyond 12 months age, the difference gradually diminished, and the values tended to converge. These phenomena are speculated to be associated with the aging process in the control group.

Table 1. The values of a-wave and b-wave of DBA/2J and DBA/2N

A wave(μ W)	DBA/2J	DBA/2N	<i>p</i>
1M	-49.2 \pm 26.3(7)	-62.6 \pm 8.4(3)	0.17
3M	-66.5 \pm 47.3(4)	-54.3 \pm 17.5(5)	0.35
6M	-56.2 \pm 12.6(4)	-75.1 \pm 25.8(3)	0.20
9M	-48.6 \pm 22.6(3)	-51.9 \pm 25.8(12)	0.43
12M	-56.9 \pm 32.8(7)	-56.9 \pm 6.3(4)	0.50
15M	-59.7 \pm 26.2(7)	-59.2 \pm 27.7(7)	0.49
B wave(μ W)	DBA/2J	DBA/2N	<i>P</i>
1M	100.2 \pm 18.2(7)	110.1 \pm 18.1(3)	0.28
3M	105.3 \pm 59.0(4)	94.5 \pm 47.3(5)	0.40
6M	91.4 \pm 22.1(4)	107.9 \pm 44.2(3)	0.33
9M	81.3 \pm 32.8(3)	96.3 \pm 26.7(12)	0.31
12M	91.7 \pm 37.7(7)	94.7 \pm 30.4(4)	0.46
15M	98.7 \pm 38.9(7)	93.7 \pm 27.8(7)	0.40

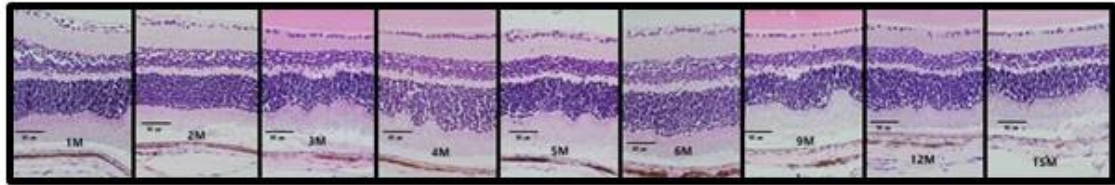
Table 2. The thickness of inner retinal layers of OCT data from DBA/2N and DBA/2J

Inner retinal layer	DBA/2J	DBA/2N	<i>p</i>
1M	68.4 \pm 3.6 (6)	62.6 \pm 2.8 (4)	<0.05
3M	72.4 \pm 1.6 (3)	66.9 \pm 2.2 (2)	0.08
6M	60.6 \pm 0.6 (2)	58.5 \pm 13.5 (9)	0.436
9M	66.7 \pm 0.2 (2)	66.1 \pm 5.0 (11)	0.372
12M	80.8 \pm 0.4 (2)	69.2 \pm 5.2 (4)	<0.05

Table 3. The thickness of total retinal layers of OCT data from DBA/2N and DBA/2J

Total retinal layer	DBA/2J	DBA/2N	<i>p</i>
1M	199.0 \pm 11.0 (6)	213.6 \pm 10.6 (4)	0.05
3M	206.8 \pm 7.1 (3)	208.6 \pm 1.2 (2)	0.38
6M	206.4 \pm 0.3 (2)	199.9 \pm 12.2 (9)	0.08
9M	217.3 \pm 13.1 (2)	206.7 \pm 12.2 (11)	0.29
12M	210.3 \pm 5.6 (2)	222.0 \pm 9.5 (4)	0.12

DBA/2J



DBA/2N

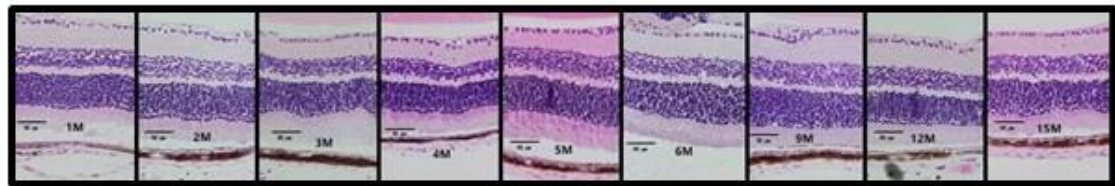


Figure 11. H&E staining samples from eye samples of DBA/2J and DBA/2N. These samples were gained from each individual in identical age of two other groups. As it seen, the thickness of retinal layers was not shown distinct changes in both groups.

Discussion

When comparing the anterior segment of control group DBA/2N and DBA/2J mice, the following abnormal changes on the retina were observed in DBA/2J mice. It had three main phenotypic features: (i) iris border thickening, (ii) pigment dispersion and (iii) pupil position alteration.

Thickening of the peripheral border of the iris was observed, which began to appear abnormally at around after 4 months age. This led to a significantly reduced extent of pupil dilation 5 minutes after anesthesia. These changes appear to worsen with age, as indicated by the increasing conformational changes in the iris. Some DBA/2J individuals exhibited pigment dispersion on the iris and partial transparency on that. This sometimes led to pupil obstruction by detached pigments, predominantly thickening in the area surrounding the pupil.

Also, the position of the pupils of DBA/2J mice eyes were altered. DBA/2J mice showed a change in pupil position, primarily shifting toward the superior-temporal side, in conjunction with the abnormal iris changes. It seemed to develop iris atrophy. In contrast, the control group DBA/2N exhibited no such abnormal findings, and the position of the pupil remained normal. These three characteristics made challenges when conducting OCT, fundus, and ERG tests on the glaucomatous mouse subjects.

In addition, both the experimental and control groups exhibited the presence of white deposits in the cornea. These deposits resembled calcifications and worsened with age, at times bulging beyond the eye. The corneal changes were mainly located in the center of the eye and above the pupil and, in severe cases, were associated with IOP.

DBA/2J mice displayed a progressive narrowing of the anterior chamber angle as they aged, a change not observed in the control group. This angle narrowing began at approximately 3 months of age, particularly in individuals exhibiting inflammatory responses in the iris. The inflammatory response is suspected to be the cause of the anterior angle closure. DBA/2J mice also showed eye swelling due to impeded drainage of aqueous humor, resulting in the widening of the pupil and cornea, which was severe enough that it was challenging to capture using OCT imaging. Additionally, changes in iris inflammation were associated with adhesions between the cornea and iris, complicating the observation of the scleral spur and causing issues in measuring the angle-opening distance (AOD), which is used for quantifying glaucomatous symptom in human patients⁹. In the measurement of AOD, it is essential to represent the area up to a specific distance from the precise location of the scleral spur¹⁷. However, due to the significant variation in the accuracy of scleral spur positioning and the patterns observed in glaucomatous individuals, it is speculated that utilizing this parameter may be faced with challenges.

Furthermore, in the ERG data, there appeared to be differences between the two groups at specific ages. However, when extrapolating from subsequent results, it seemed that such differences diminished. Therefore, it is suggested that additional experiments are required to determine if this can serve as a standard for glaucoma-related experiments using DBA/2J. Despite the results obtained from the ERG data, H&E staining results might show different possibilities, conducting thickness analysis, therefore we carried out the procedures. However, as shown in figure 11, it might be challenging to claim clear-cut results from these analyses¹⁸.

Perhaps, when considering the glaucoma-related characteristics of DBA/2J, the focus should primarily revolve around changes in the conformational changes on anterior segment, anterior angle closure, and the IOP increase related with ages.

References

1. Jonas JB, Aung T, Bourne RR, Bron AM, Ritch R, Panda-Jonas S. Glaucoma. *Lancet*. 2017 Nov 11;390(10108):2183-2193. doi: 10.1016/S0140-6736(17)31469-1. Epub 2017 May 31. PMID: 28577860.
2. Tham YC, Li X, Wong TY, Quigley HA, Aung T, Cheng CY. Global prevalence of glaucoma and projections of glaucoma burden through 2040: a systematic review and meta-analysis. *Ophthalmology*. 2014 Nov;121(11):2081-90. doi: 10.1016/j.ophtha.2014.05.013. Epub 2014 Jun 26. PMID: 24974815.
3. Yücel YH, Zhang Q, Gupta N, Kaufman PL, Weinreb RN. Loss of neurons in magnocellular and parvocellular layers of the lateral geniculate nucleus in glaucoma. *Arch Ophthalmol*. 2000 Mar;118(3):378-84. doi: 10.1001/archopht.118.3.378. PMID: 10721961.
4. Crawford ML, Harwerth RS, Smith EL 3rd, Mills S, Ewing B. Experimental glaucoma in primates: changes in cytochrome oxidase blobs in V1 cortex. *Invest Ophthalmol Vis Sci*. 2001 Feb;42(2):358-64. PMID: 11157867.
5. Sample PA, Bosworth CF, Blumenthal EZ, Girkin C, Weinreb RN. Visual function-specific perimetry for indirect comparison of different ganglion cell populations in glaucoma. *Invest Ophthalmol Vis Sci*. 2000 Jun;41(7):1783-90. PMID: 10845599.
6. Turner AJ, Vander Wall R, Gupta V, Klistorner A, Graham SL. DBA/2J mouse model for experimental glaucoma: pitfalls and problems. *Clin Exp Ophthalmol*. 2017 Dec;45(9):911-922. doi: 10.1111/ceo.12992. Epub 2017 Jun 13. PMID: 28516453.
7. Steele MR, Inman DM, Calkins DJ, Horner PJ, Vetter ML. Microarray analysis of retinal gene expression in the DBA/2J model of glaucoma. *Invest Ophthalmol Vis Sci*. 2006 Mar;47(3):977-85. doi: 10.1167/iovs.05-0865. PMID: 16505032.
8. Wilson GN, Inman DM, Dengler Crish CM, Smith MA, Crish SD. Early pro-inflammatory cytokine elevations in the DBA/2J mouse model of glaucoma. *J Neuroinflammation*. 2015 Sep 17;12:176. doi: 10.1186/s12974-015-0399-0. Erratum in: *J Neuroinflammation*. 2015;12:191. Denger-Crish, Christine M [corrected to Dengler Crish, Christine M]. PMID: 26376776; PMCID: PMC4574349.
9. Aihara M, Lindsey JD, Weinreb RN. Twenty-four-hour pattern of mouse intraocular

pressure. *Exp Eye Res.* 2003 Dec;77(6):681-6. doi: 10.1016/j.exer.2003.08.011. PMID: 14609556.

10. Wang J, Dong Y. Characterization of intraocular pressure pattern and changes of retinal ganglion cells in DBA2J glaucoma mice. *Int J Ophthalmol.* 2016 Feb 18;9(2):211-7. doi: 10.18240/ijo.2016.02.05. PMID: 26949637; PMCID: PMC4761729.
11. Chrysostomou V, Valter K, Stone J. Cone-rod dependence in the rat retina: variation with the rate of rod damage. *Invest Ophthalmol Vis Sci.* 2009 Jun;50(6):3017-23. doi: 10.1167/iovs.08-3004. Epub 2009 Jan 31. PMID: 19182251. John SW, Smith RS, Savinova OV, Hawes NL, Chang B, Turnbull D, Davisson M, Roderick TH, Heckenlively JR. Essential iris atrophy, pigment dispersion, and glaucoma in DBA/2J mice. *Invest Ophthalmol Vis Sci.* 1998 May;39(6):951-62. Erratum in: *Invest Ophthalmol Vis Sci* 1998 Aug;39(9):1641. PMID: 9579474.
12. John SW, Smith RS, Savinova OV, Hawes NL, Chang B, Turnbull D, Davisson M, Roderick TH, Heckenlively JR. Essential iris atrophy, pigment dispersion, and glaucoma in DBA/2J mice. *Invest Ophthalmol Vis Sci.* 1998 May;39(6):951-62. Erratum in: *Invest Ophthalmol Vis Sci* 1998 Aug;39(9):1641. PMID: 9579474.
13. Anderson MG, Smith RS, Hawes NL, Zabaleta A, Chang B, Wiggs JL, John SW. Mutations in genes encoding melanosomal proteins cause pigmentary glaucoma in DBA/2J mice. *Nat Genet.* 2002 Jan;30(1):81-5. doi: 10.1038/ng794. Epub 2001 Dec 17. PMID: 11743578.
14. Inman DM, Sappington RM, Horner PJ, Calkins DJ. Quantitative correlation of optic nerve pathology with ocular pressure and corneal thickness in the DBA/2 mouse model of glaucoma. *Invest Ophthalmol Vis Sci.* 2006 Mar;47(3):986-96. doi: 10.1167/iovs.05-0925. PMID: 16505033.
15. Libby RT, Anderson MG, Pang IH, Robinson ZH, Savinova OV, Cosma IM, Snow A, Wilson LA, Smith RS, Clark AF, John SW. Inherited glaucoma in DBA/2J mice: pertinent disease features for studying the neurodegeneration. *Vis Neurosci.* 2005 Sep-Oct;22(5):637-48. doi: 10.1017/S0952523805225130. PMID: 16332275.
16. Rohowetz LJ, Mardelli ME, Duncan RS, Riordan SM, Koulen P. The Contribution of Anterior Segment Abnormalities to Changes in Intraocular Pressure in the DBA/2J Mouse Model of Glaucoma: DBA/2J-Gpnm^b+ /SJJ Mice as Critical Controls. *Front*

Neurosci. 2022 Feb 3;15:801184. doi: 10.3389/fnins.2021.801184. PMID: 35185449; PMCID: PMC8850401.

17. John SW, Smith RS, Savinova OV, Hawes NL, Chang B, Turnbull D, Davisson M, Roderick TH, Heckenlively JR. Essential iris atrophy, pigment dispersion, and glaucoma in DBA/2J mice. *Invest Ophthalmol Vis Sci*. 1998 May;39(6):951-62. Erratum in: *Invest Ophthalmol Vis Sci* 1998 Aug;39(9):1641. PMID: 9579474.
18. Pakuliene G, Zimarinas K, Nedzelskiene I, Siesky B, Kuzmiene L, Harris A, Januleviciene I. Anterior segment optical coherence tomography imaging and ocular biometry in cataract patients with open angle glaucoma comorbidity. *BMC Ophthalmol*. 2021 Mar 8;21(1):127. doi: 10.1186/s12886-021-01874-x. PMID: 33685443; PMCID: PMC7941888.

국문 초록

녹내장이란 비정상적 안압과 연관된 시신경 퇴행성 질환으로써 안구 내 순환하는 방수의 비정상적 생성과 유출에 연관되어 있다. 생성되는 양이 비정상적으로 많아지거나, 전방각이 막혀서 방수량이 심각히 늘어나면 안압이 비정상적으로 증가하게 된다. 이로 인해 망막층과 시신경이 영향을 받기 때문에 변성이 일어나게 된다. 특히나 신경절 세포층에 피해를 주는 것으로 알려져 있다. 전 세계적으로 40대와 60대 사이에 약 3.54%의 발병률을 띤다.

녹내장에 대한 실험을 진행함에 앞서, 실험군으로 쓰이는 DBA/2J의 표현형 분석을 진행하고자 했다. 기존에 해당 계열군의 특징으로 보고된 것은, 3개월령에서 6개월령의 기간 동안 홍채 위축과 탈색소화, 전안부 개방각의 닫힘 현상과 그로 인한 것으로 추측되는 안압 (intraocular pressure; IOP)의 비정상적인 증가, 그리고 이후 녹내장성 망막층의 변성이 있다. 이 실험군 개체들의 제어군으로는 같은 계열에 속하는 DBA/2N이 사용되었으며, 1개월령부터 15개월령까지의 관찰이 이루어졌다.

우리는 해당 현상들의 발현을 확인하기 위해 여러가지 관찰을 진행했다. 전안부 촬영을 통한 홍채 위축과 탈색소화 관찰, 안압 측정기를 활용한 안압 측정, 빛간섭 단층 촬영(ocular coherence; OCT)과 망막전위도검사(electroretinography; ERG)를 활용한 전안부 개방각과 망막층의 관찰, 그리고 H&E 조직염색법을 통한 망막내부층 두께변화 관찰 등이 있었다.

실험의 결과로 전안부 촬영에서는 뚜렷한 변화가 보였다. DBA/2J에서는 홍채의 변화가 3개월령 이후로 나타나기 시작했으며 홍채 외각의 두께가 비이상적으로 두꺼워지거나, 동공의 크기변화가 점차 사라지는 등의 형태를 드러냈다. 또한 염증으로 인한 것으로 추측되는 탈

색소화로 인해, 동공에 해당 색소들이 끼어들어가 차후 다른 관찰에 있어서 장애가 되기도 하였다. 그런 변화가 나타난 개체로부터 얻어낸 IOP 데이터도 제어군과는 뚜렷한 차이를 보였으며(15개월령 양안 IOP 평균 DBA/2N: 약 12.3 mmHg, DBA/2J: 17.3mmHg), 이후에 이뤄진 전안부 개방각의 폐쇄여부를 확인한 OCT 데이터에서도 실험군에서 더 명확한 결과를 나타냈다. 하지만 그와 같이 수행된 다른 검사들의 결과에서는 뚜렷한 차이를 드러내지 못했다. ERG는 a-wave와 b-wave 모두 실험군과 제어군에서 확연한 값의 차이를 보이지 못했다(12개월령에서 a-wave - DBA/2J: -56.9 ± 32.8 , DBA/2N: -56.9 ± 6.3 / b-wave - DBA/2J: 91.7 ± 37.7 , DBA/2N: 94.7 ± 30.4). 망막 두께분석에서 전체 망막층은 연령대에 따른 두께변화가 조금 있었지만 내부 망막층에서는 연령대에 따른 변화도 잘 보이지 않았다. H&E 조직염색도 결과에서 연령대에 따른 변화도 뚜렷하게 보이지 않았다.

결과를 비추어 보아, DBA/2J에서 녹내장성의 증상이 발현되는 것은 일부적으로 맞는 것으로 보였다. 이러한 증상들은 홍채위축과 탈색소화 그리고 전방 개방각의 폐쇄 등을 포함하였으며, 이로 인한 것으로 추측되는 IOP 증가가 있다. 하지만 또한 기존에 보고된 바와 같이 망막 내부의 신경절 세포층 두께 변화와 같은 변성에 대한 결과는 뚜렷할 만한 차이가 나지 않았다. 또한 전안부의 변화에 있어서도 실험에 장애가 될 사항들이 나타났는데, 탈색소화로 인한 변화에서 동공이 가로 막히는 것과 각막의 변화였다. 특히, 각막의 변화는 안구의 중심부 근에 나타나서 혈관이 생성되는 등의 상태까지 나타났는데 이로 인해 동공이 가로막히는 것은 물론, IOP 측정에서도 장애요소가 되었다. 동공이 가로막혀 OCT, ERG 등의 실험장치를 통한 관찰이 불가능한 개체들도 있었다. 따라서 DBA/2J의 녹내장 질환 연구 사용에 있어서는 추가적인 연구가 필요할 것으로 결론 내리게 되었다.